J. Membrane Biol. 196, 105–116 (2003)
DOI: 10.1007/s00232-003-0629-8

The Journal of
Membrane
Biology

Interpretation and Optimization of Absorbance and Fluorescence Signals from Voltage-sensitive Dyes

P.Y. Chang, M.B. Jackson
Department of Physiology and Biophysics Ph.D. Program, University of Wisconsin, Madison WI 53706, USA

Received: 26 June 2003/Revised: 10 September 2003

Abstract. Voltage-sensitive dyes produce absorbance and fluorescence changes that can be used to image voltage. The present study develops a systematic approach to the optimization of these signals. A mathematical analysis assesses the dye optical density (*OD*) that optimizes the signal-to-noise ratio in absorbance and fluorescence measurements. The signal-to-noise ratio is maximal for a dye *OD* of 2 (natural logarithm) in absorbance and ~1 in fluorescence. The fluorescence result is approximate because, in contrast to absorbance, the optimal dye *OD* varies with the amount of scattering and intrinsic absorbance of the tissue. The signal-to-noise ratio of absorbance is higher in thick preparations such as brain slices; fluorescence is superior in thin preparations such as cell culture. The optimal *OD* for absorbance and fluorescence, as well as the superiority of absorbance, were confirmed experimentally on hippocampal slices. This analysis also provided insight into the interpretation of signals normalized to resting light intensities. With both absorbance and fluorescence, the normalized signal ($\Delta I/I$) varies with *OD*, and does not reflect the change in dye absorbance. In absorbance this problem is remedied by dividing $\Delta I/I$ by the dye *OD* to obtain the absorbance change. For fluorescence a correction is possible, but is more complicated. Because this analysis indicates that high levels of stain optimize the signal-to-noise, dyes were tested for pharmacological actions and phototoxicity. The absorbance dye RH155 was found to have pharmacological action at high staining levels. The fluorescent dye RH414 was phototoxic. Adverse effects could not be detected with the absorbance dye RH482.

Key words: Voltage imaging — Styryl dyes — Electrochromic dyes — Neural imaging

Correspondence to: M.B. Jackson; email: mjackson@physiology.wisc.edu

Introduction

Voltage-sensitive dyes provide an optical signal suitable for imaging voltage in living tissue. These dyes serve as powerful tools in the study of electrical activity in the nervous system as well as in other electrically excitable tissue (Cohen & Salzberg, 1978; Grinvald et al., 1988; Kamino, 1991; Salzberg, 1983; Wu and Cohen, 1993). A significant limitation in voltage-imaging research is the quality of the dyes, and considerable effort has been devoted to their development and characterization. Extensive screening studies have identified a number of dyes that change their absorbance or fluorescence in response to membrane potential and are suitable for imaging voltage in various tissues (Ross et al., 1977; Ross et al., 1997; Gupta et al., 1981; Fluher, Burnham & Loew, 1985; Grinvald et al., 1988; Momose-Sato et al., 1999; Shoham et al., 1999). However, once suitable dyes are found, attention must be directed toward optimizing conditions for their use. This is usually done empirically, with dye concentration and staining time varied until an acceptable result is obtained. A more systematic approach to the optimal use of voltage-sensitive dyes would help investigators, both in comparing and evaluating dyes as well as in designing experiments.

The use of voltage-sensitive dyes is further limited by uncertainty in the interpretation of measured signals (Grinvald et al., 1988). It is virtually impossible to quantitate amplitudes of voltage changes across a cell membrane with a voltage-sensitive dye because signals represent a complex weighted sum of signals from dye residing in the membranes of the various cells within an elementary imaging element or pixel. Signals vary with tissue thickness, dye density, illumination intensity, and a variety of other experimental parameters. In an effort to reduce the impact of these various parameters it is common practice to normalize observed signals to the resting light inten-

sity. The normalized change, $\Delta I/I$, is expected to bear a closer relation to the average absorbance change, $\Delta A/A$, and the absorbance change is a more fundamental quantity that should provide a better measure of aggregate electrical activity at an imaged site. Dividing by the resting light has a seductive appeal in giving a quantity thought to be more reliable and less sensitive to some of the less relevant details of experiments. A change in absorbance will produce a change in the opposite direction for a transmitted light signal and a change in the same direction for a fluorescent light signal. Fluorescent dyes that do not change their quantum yield should report just the change in absorbance. However, for both fluorescence and absorbance dyes the relation between $\Delta I/I$ and changes in dye properties is not well understood.

A better understanding of theoretical aspects of voltage sensitive dyes will greatly facilitate the development of dyes and the design of experiments (Waggoner, 1979). The present study addresses these issues along three lines. (1) A systematic approach to the optimization of staining conditions is developed for voltage imaging experiments. (2) The relationship is explored between normalized changes in light intensity and the actual absorbance change of an optical probe. (3) Comparisons are made between absorbance and fluorescence to evaluate their relative merits as readouts of electrical activity.

Materials and Methods

Experiments

Voltage-imaging experiments employed the same instrumentation used in previous reports from this laboratory (Jackson & Scharfman, 1996; Demir, Haberly & Jackson, 1998). The instrumentation follows Wu and Cohen (1993) and is very similar to the commercial photodiode system Neuroplex-II from RedShirtImaging LLC (Fairfield, CT). Signals were recorded with a 464-element hexagonal photodiode array, amplified to 0.5–200 V/pA of photocurrent, low-pass filtered at 500 Hz, and read into a PC. In some experiments signals were high-pass filtered with a time constant of 500 msec. Data acquisition and analysis were performed with an in-house computer program written in C. Additional analysis and plotting were performed with the computer program Origin (Microcal, Northampton, MA).

Light recording employed either a 5× fluar objective (Zeiss, numerical aperture NA = 0.25), a 10× fluar objective (Zeiss, NA = 0.50), or a 20× xLUMPLfl objective (Olympus, NA = 0.95). The preparation was illuminated from below with a 100 W halogen bulb through a 702 ± 18 nm bandpass filter (Omega, Brattleboro VT) for RH155 and RH482 and a 520 ± 45 nm bandpass filter (Chroma, Brattleboro VT) for RH414. In absorbance measurements with RH414, collected light was filtered again with a 520 ± 45 nm bandpass filter to remove fluorescent light (transmission filter). Fluorescence recording generally employed the same illumination as absorbance. Collected light was passed through a 590 nm dichroic mirror and a 610 nm longpass filter (emission filter). Absorbance and fluorescence were recorded alternately from the same preparation with the same stimulation by exchanging filters above the objective (Fig. 1). It should be noted that because RH414 is strongly

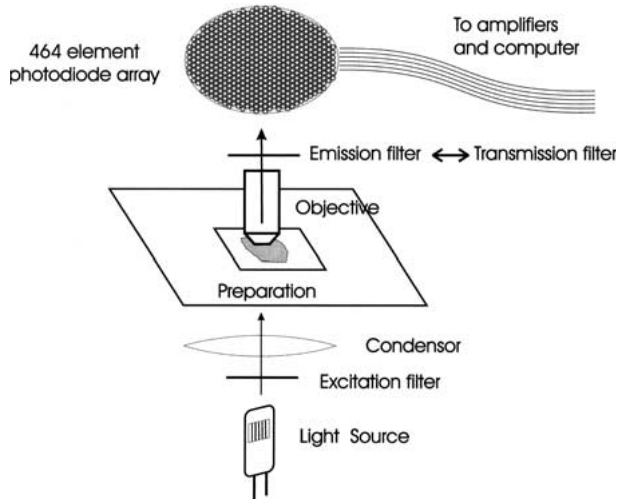

Fig. 1. A sketch of the voltage-imaging system used in this study. The same dye could be tested for absorbance and fluorescence in the same experiment by switching between the transmission and emission filters to select light of the same wavelength as that used for excitation, or for light at the emission wavelength.

fluorescent, removing the fluorescent light with the 520 ± 45 nm bandpass filter above the objective was essential to obtain meaningful absorbance measurements. Without this filter, signals were an uninterpretable mixture of fluorescent and transmitted light.

Hippocampal slices (300–400 μm) were prepared by standard methods from rats ~2 months old. Dissection and recording were performed in artificial cerebrospinal fluid (aCSF) consisting of (in mM) 125 NaCl, 4 KCl, 1.25 NaH_2PO_4, 26 $NaHCO_3$, 2 $CaCl_2$, 1 $MgSO_4$ and 10 glucose, bubbled with 95% O_2/5% CO_2. Slices were stained with either RH414 (0.2 mM), RH155 (0.2 mg/ml) (Molecular Probes, Eugene OR), or RH482 (0.2 mg/ml) (NK3630, Hayashibara Biochemical Laboratories, Okayama, Japan). To vary the staining level, slices were left in staining solution for times varying from 10–90 minutes. Electrical stimulation was applied as a 0.1–0.2 msec, 10–200 μA shock from a stimulus isolator through a glass micropipette filled with aCSF. Field potentials were recorded with patch electrodes filled with aCSF, using an Axopatch 1C amplifier (Axon Instruments, Foster City, CA). Stimulus artifacts were removed from field-potential recordings for display.

Responses were averages of 1–10 trials at 5-second intervals. Resting light intensities and peak stimulus-evoked changes were measured and analyzed as indicated in Results. The present analysis depends on determination of A, the optical density (OD) of the dye in a slice. Here we found it more convenient to define the OD in terms of the natural logarithm rather than $\log_{10}$. First we measured the light detected at two central detectors under the conditions of an experiment, with no tissue in the light path. This quantity is referred to as I_0. The OD of an unstained slice, S, was then determined by making the same measurement with an unstained slice in the light path. This gave I_0e^{-S} (*see* Theory), allowing the calculation of S. Two or three unstained slices were measured each day of an experiment in which OD data was determined. S was then used in Eq. 3 (given below), to solve for A from a measurement of the recorded light intensity of a stained slice.

Theory

The analysis here will consider signals resulting from a change in dye absorbance within the illumination bandwidth. For electro-

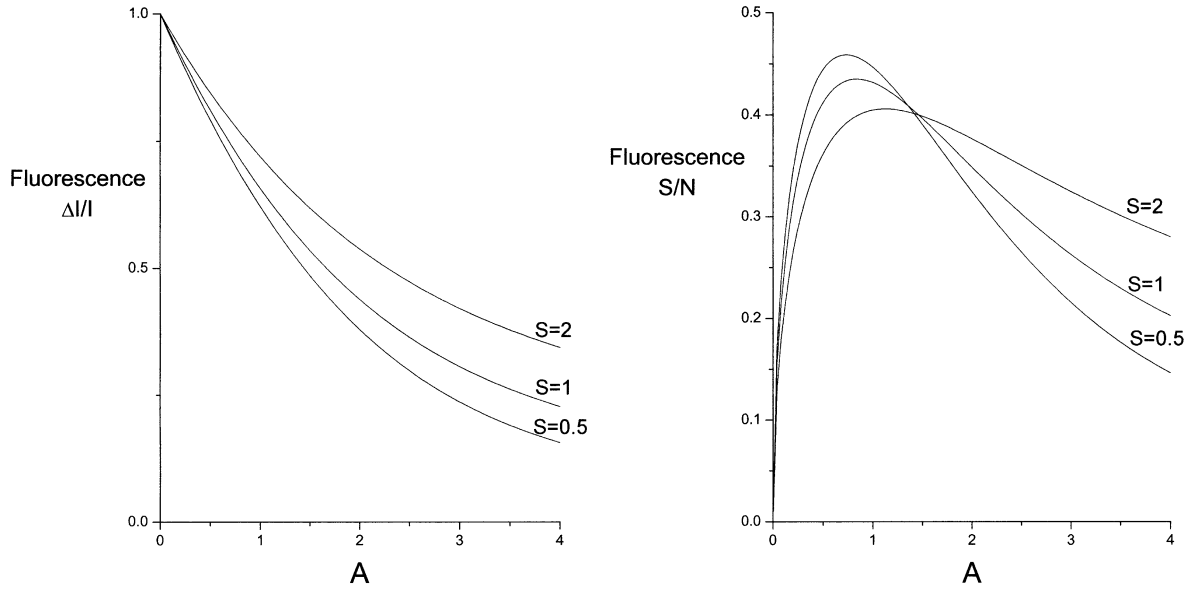

Fig. 2. Plots of Eq. 11 (*A*) and Eq. 12 (*B*). As A (dye OD) increases, Eq. 11 shows that the normalized signal $\Delta I_f/I_f$ declines monotonically for various values of S. Equation 12 shows that the signal-to-noise ratio peaks around $A \sim 1$, with some variation depending on S.

chromic dyes the change is due to a shift in the absorbance spectrum (Waggoner, 1979; Loew et al., 1985), but the present analysis does not depend on the mechanism by which the absorbance change is produced. The analysis of fluorescence is based on the assumption that fluorescence signals report only changes in dye absorbance. The quantum yield, Q, is assumed to remain constant, although some electrochromic dyes appear to show changes in Q as well (Fluhler et al., 1985).

Because the environment of the dye molecules varies, the extinction coefficient is heterogeneous. We thus define the OD of the dye, denoted as A,

$$A = \sum_{i=1}^{N} \varepsilon_i(V_i) \tag{1}$$

for a region containing N dye molecules. $\varepsilon_i(V_i)$ reflects the extinction coefficient of molecule i residing in a particular membrane with voltage V_i. An electrical stimulus applied to the preparation will evoke a change in A that reflects the aggregate change in all the $\varepsilon_i(V_i)$. The theoretical analysis here will take the quantity ΔA as the change in A resulting from a stimulus. If we consider varying staining conditions so that the density of dye in the tissue is varied, but the distribution between different environments remains the same, then the fractional change in absorbance, $\Delta A/A$, can be treated as an indicator of electrical activity from that site. The quantity $\Delta A/A$ is thus a fundamental characteristic of an electrical response. We will pose the following questions about $\Delta A/A$: (1) How do changes in measured transmitted and fluorescent light relate to $\Delta A/A$? and (2) How does one optimize the signal-to-noise ratio with respect to dye staining?

Absorbance

In an absorbance experiment, the transmitted light is imaged. In a preparation of living tissue, an infinitesimally thin layer will absorb a fraction of light proportional to the thickness of the layer. For a layer at vertical position x, the light absorbed by the dye is $-I(x)\alpha dx$, and the light absorbed by the tissue (intrinsic absorbance and scattering) is $-I(x)\sigma dx$. α and σ are ODs per unit path length; α is proportional to the density of dye in the tissue. Assuming that these two parameters are uniform with respect to x leads to an expression for the recorded light signal, I_r.

$$I_r = I_0 e^{-(\sigma+\alpha)t} \tag{2}$$

t is the thickness of the tissue, and as mentioned before, I_0 is the light intensity recorded in the absence of tissue. Eq. 2 is the counterpart to the Beer-Lambert law for a slice of tissue stained with an absorbent dye. Since α and σ are ODs per unit path length, we can replace σt by S and αt by A.

$$I_r = I_0 e^{-(S+A)} \tag{3}$$

Eq. 3 illustrates the convenience of our choice to define the OD in terms of the natural logarithm of measured light intensity rather than the more commonly used $\log_{10}$.

Now we estimate how the signal I_r changes when a stimulus is applied such that A changes by an amount ΔA. Electrochromic dyes generally give small fractional changes, so that ΔI_r is well approximated as

$$\begin{aligned}\Delta I_r &= \frac{dI_r}{dA}\Delta A = \frac{d(I_0 e^{-(S+A)})}{dA}\Delta A \\ &= -I_0 e^{-(S+A)}\Delta A\end{aligned} \tag{4}$$

Normalizing this signal to the resting light intensity is accomplished by dividing by Eq. 3.

$$\frac{\Delta I_r}{I_r} = -\Delta A \tag{5}$$

Since the goal is to relate this to the more fundamental quantity $\Delta A/A$, we divide by A

$$\frac{1}{A}\frac{\Delta I_r}{I_r} = -\frac{\Delta A}{A} \tag{6}$$

This result provides an important insight into the interpretation of signals based on absorbance changes. The normalized change in recorded light depends on the amount of bound dye (Fluhler et al., 1985), and is a different quantity from the normalized change in the absorbance of the dye. In order to relate $\Delta I_r/I_r$ to $\Delta A/A$, we must divide it by A. A will increase with dye density, but the quantity

$\Delta A/A$ should remain constant. So the measured $\Delta I_r/I_r$ will have a linear relation with A, and this can be corrected for by measuring A and dividing. This relation will be tested experimentally in Results.

Seeing that staining with more dye gives larger normalized signals might imply that experimenters should stain the tissue with as much dye as possible. However, this reduces the intensity of the light signal (and may have pharmacological effects as well). When the noise in a recording is due to photon shot noise, as is often the case in voltage-imaging experiments (Salzberg, 1983; Cohen & Lesher, 1986; Grinvald et al., 1988; Wu et al., 1998; Jin, Zhang & Wu, 2002), then reducing the intensity of the signal will also reduce the signal-to-noise ratio. This suggests that there is an optimal staining density at which the signal-to-noise ratio is maximized. This maximum is derived as follows.

It is convenient to define light intensity in units of photons striking the detector per sampling interval. The variance in this number is simply the square root, so the noise (RMS) is given by $\sqrt{I_r}$. Taking I_r from Eq. 3, and the measured change in light intensity from Eq. 4, we obtain the signal-to-noise ratio as

$$S/N = \frac{I_0 e^{-(A+S)}|\Delta A|}{\sqrt{I_0 e^{-(A+S)}}} = \frac{|\Delta A|}{A}\sqrt{I_0 e^{-S}}\,A e^{-A/2} \tag{7}$$

$\Delta A/A$ is factored out in front because this is taken as a fundamental quantity independent of dye density. Treating $\Delta A/A$ as invariant means that to optimize the signal-to-noise ratio we should focus on

$$S/N \propto A e^{-A/2} \tag{8}$$

This expression has a maximum of 0.74 at $A = 2$. Thus, the signal-to-noise will be optimized when the tissue is stained to a degree such that dye absorbance reduces the transmitted light by the fraction $e^{-2} = 0.135$ of that of unstained tissue. This result had been obtained previously (B. M Salzberg, L. B. Cohen, and W. N. Ross, personal communication), and is generally applicable to absorbance measurements for the case where photon shot noise predominates over other sources of noise (Skoog, 1985).

Fluorescence

This analysis can be extended to fluorescence changes. For the sake of comparison with the foregoing analysis of absorbance, we envisage the fluorescence imaging experiment in a transmission mode (diascopic), with illumination through a condenser and fluorescent light captured by a microscope objective (Fig. 1). This contrasts with the almost universal use of epifluorescence in fluorescence microscopy. Thus, an emission filter is placed above the objective as in epifluorescence, but the excitation filter is placed below the condenser, as in an absorbance experiment. Because the illumination source in diascopic fluorescence is the same as that in absorbance, fluorescence in this configuration has the advantage of being more easily compared to absorbance. A comparable analysis can be performed of epifluorescent illumination, but the comparison with absorbance measurements would then require a quantitative calibration of two different light sources and optical pathways.

If the light illuminating the preparation is denoted as I_{ill} (a relation between I_{ill} and I_0 will be indicated below), then the light transmitted through the preparation has the same proportion seen in Eq. 3

$$I_{trans} = I_{ill} e^{-(A+S)} \tag{9}$$

Of the light not transmitted, $(I_{ill} - I_{trans}) = I_{ill}(1 - e^{-(A+S)})$, a fraction $A/(A+S)$ is absorbed by the dye. (This is true even if α and σ vary with x, provided that they vary in parallel). The fluorescence equals this absorbed fraction multiplied by the quantum yield of the dye (denoted as Q). The detected fluorescence is then obtained by multiplying by a geometric factor (denoted as ζ) that gives the fraction of emitted light collected by the objective. (ζ will be calculated below for the comparison of fluorescence and absorbance.) The recorded fluorescent light signal is

$$I_f = I_{ill} Q \zeta \frac{A}{A+S}(1 - e^{-(A+S)}) \tag{10}$$

To obtain the electrically evoked change in fluorescence, ΔI_f, we once again differentiate with respect to A. By the same method used to obtained $\Delta I_r/I_r$ above, we obtain

$$\frac{\Delta I_f}{I_f} = \left(\frac{\Delta A}{A}\right)\left(\frac{A e^{-(A+S)}}{1 - e^{-(A+S)}} + \frac{S}{A+S}\right) \tag{11}$$

and for the signal-to-noise ratio

$$S/N = \left(\frac{|\Delta A|}{A}\right)\frac{\sqrt{\frac{I_{ill} Q \zeta A}{A+S}}\left(A e^{-(A+S)} + \frac{S}{A+S}(1 - e^{-(A+S)})\right)}{\sqrt{1 - e^{-(A+S)}}} \tag{12}$$

In contrast to the simple formulas derived for absorbance, these formulas show a complex dependence of $\Delta I_f/I_f$ and signal-to-noise ratio on dye OD. These results will also be more difficult to use because of their dependence on S. Eqs. 11 and 12 are plotted versus A in Fig. 2. The factor $\Delta A/A$ was held at 1 under the assumption that the fractional change in dye absorbance is independent of dye OD. $I_0 Q \zeta$ was taken as 1 and S was 0.5, 1 and 2, typical values for slices of brain. Eq. 11 shows that $\Delta I_f/I_f$ declines monotonically as A increases (Fig. 2*A*). The results vary somewhat for the different values of S but the qualitative behavior is similar. Eq. 12 shows that, like the absorbance measurement, the fluorescence measurement has a specific dye OD for optimal signal-to-noise (Fig. 2*B*). However, the position of the maximum is different; values are all near $A = 1$, but vary for different values of S.

Fluorescence versus Absorbance

We will evaluate the light collected by the microscope objective in fluorescence and absorbance experiments and take this as our signal, ignoring differences in the efficiencies of the emission and transmission filters for the two experiments. To evaluate the relative performance of fluorescence and absorbance, we must first account for the different optical geometries of the two measurements. For absorbance, we picture a cone of light converging on the preparation from the condenser and an inverted cone radiating out that is collected by the microscope objective. In the absence of any absorbance by the preparation the recorded light will be related to the illuminating light by the ratio of the areas of the spherical sections of unit radius for the two respective lenses. For each lens this area is $2\pi(1-\cos\theta)$, with θ as the angle between the central optical axis and a ray along the surface of the cone. We can calculate θ from the numerical aperture of the objective since $NA = n \sin\theta$. The refractive index n is taken as one for convenience. If the illumination intensity is I_{ill}, then

$$I_0 = I_{ill}\frac{1 - \cos\theta_{obj}}{1 - \cos\theta_{cond}} \tag{13}$$

with the subscripts indicating the relevant angles for the objective and condenser. This is valid only when $\theta_{obj} < \theta_{cond}$. For fluorescence the light collected is the fraction of total light captured by the objective. Thus, we divide $2\pi(1-\cos\theta_{obj})$ by the area of a unit sphere (4π) to obtain ζ.

$$\zeta = (1 - \cos\theta_{obj})/2. \tag{14}$$

To compare the signal-to-noise ratio for fluorescence and absorbance, we substitute the expression in Eq. 13 for I_0 in Eq. 7. For $S = 1$, the maximum value of Eq. 7 is evaluated at $A = 2$ as

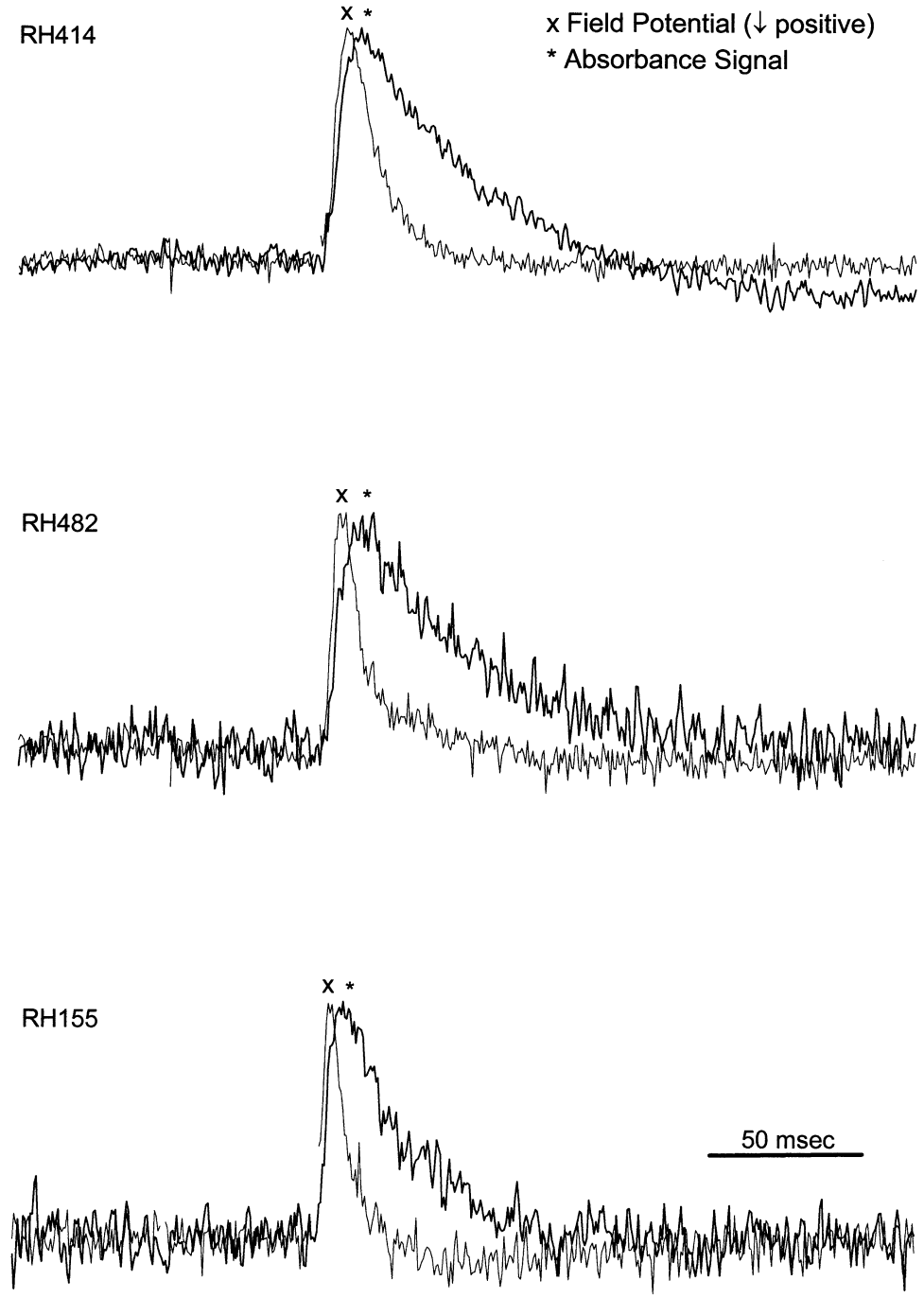

Fig. 3. Simultaneous field potentials and dye signals for slices stained with RH414, RH482, and RH155. Signals are normalized to their maxima to facilitate comparison. The field potential was negative prior to normalization. All show the general trend of peaking field potential during the rising phase of the dye signal. Small variations were seen in the decay of the field potential. Signals are averages of six trials.

$0.45\frac{|\Delta A|}{A}\sqrt{I_{\text{ill}}\frac{1-\cos\theta_{\text{obj}}}{1-\cos\theta_{\text{cond}}}}$ (0.45 was evaluated from $e^{-1/2}2e^{-1}$). The maximum value of Eq. 12 is $0.43\frac{|\Delta A|}{A}\sqrt{I_{\text{ill}}Q(1-\cos\theta_{\text{obj}})/2}$ (the value of 0.43 can be read from Fig. 2*B* for $S = 1$). Dividing these two gives the ratio of optimal signal-to-noise ratios as

$$\frac{(S/N)_{\text{f}}}{(S/N)_{\text{a}}} = 0.96\sqrt{Q(1-\cos\theta_{\text{cond}})/2} \tag{15}$$

Note that θ_{obj} does not appear in the result because it contributes equally to absorbance and fluorescence. θ_{cond} appears in the result because increasing the condenser *NA* excites more dye molecules and thus increases the fluorescence signal. By contrast, the transmitted light signal is not improved by increasing θ_{cond} when $\theta_{\text{cond}} > \theta_{\text{obj}}$.

We take $Q = 0.4$ based on measurements of several compounds used in voltage imaging (Fluher et al., 1985), and calculate θ_{cond} for a condenser *NA* of 1 to obtain 0.43 as the ratio in Eq. 15. (With a condenser *NA* of 0.9 the ratio is 0.32). Note that this result is sensitive to *S*. Repeating the calculation for $S = 2$

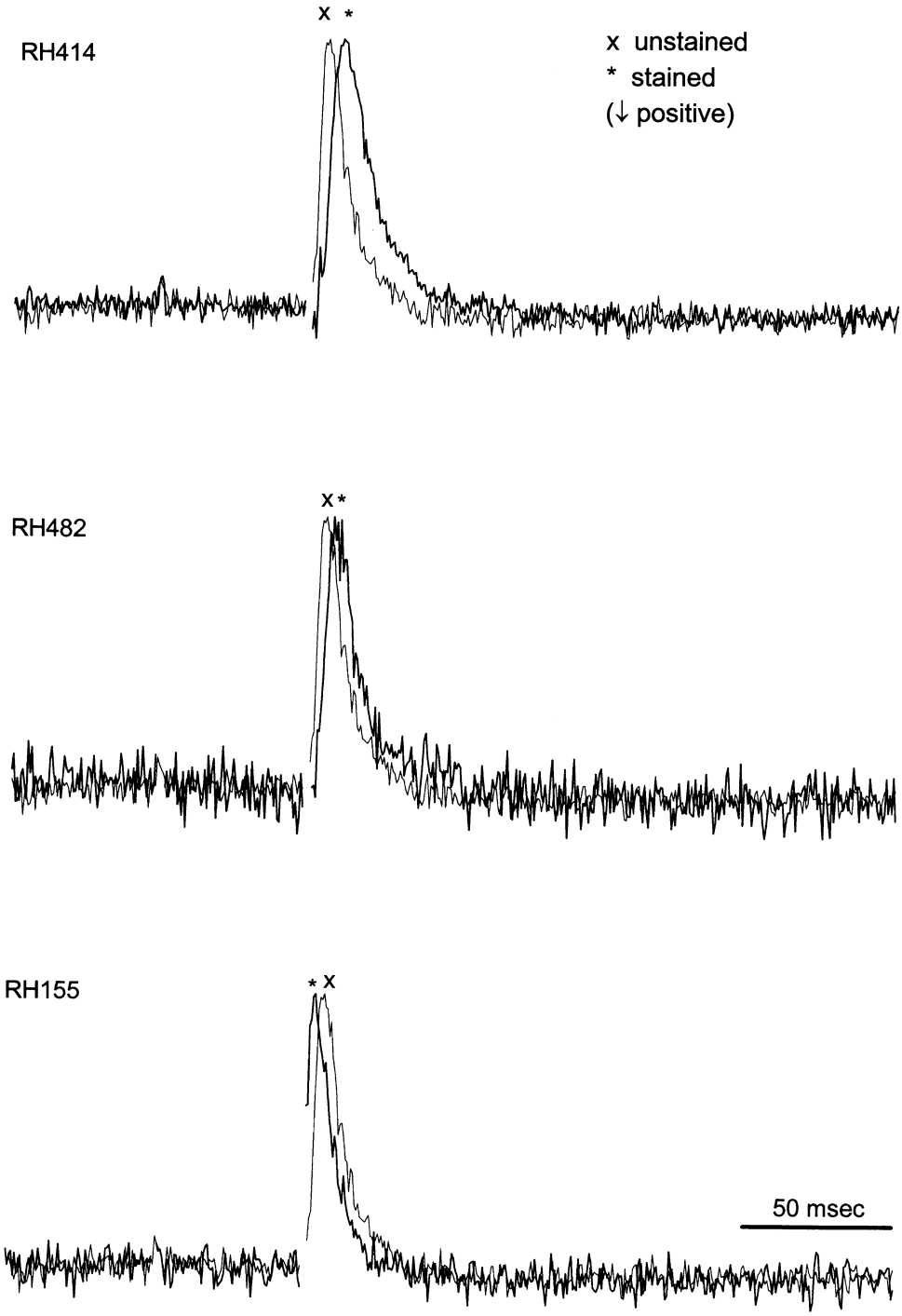

Fig. 4. Comparison of field potentials in stained and unstained slices (normalized and inverted, as in Fig. 3). Field potentials were normalized to their maxima to allow the time course to be compared. The same control trace was used for the comparison with each dye. The slight differences in latency reflect variations in distance between the stimulus and recording sites. All slices were stained lightly, for ~ 15 minutes. Signals are averages of six trials.

rather than 1 reduces the signal-to-noise ratio for absorbance by 40% but reduces the signal-to-noise ratio for fluorescence by only 5%, to give a ratio of ratios of about 0.7. This confirms that absorbance gives better signals than fluorescence in thick preparations (Cohen & Lesher, 1986; Grinvald, 1988; Wu et al., 1998; Jin et al., 2002).

When the tissue becomes very thin the tables turn in favor of fluorescence. In this case, A and S both become very small, and it can then be shown that the ratio of signal-to-noise ratios goes to

$$\frac{(S/N)_f}{(S/N)_a} \rightarrow \sqrt{\frac{Q(1-\cos\theta_{cond})}{2A}} \tag{16}$$

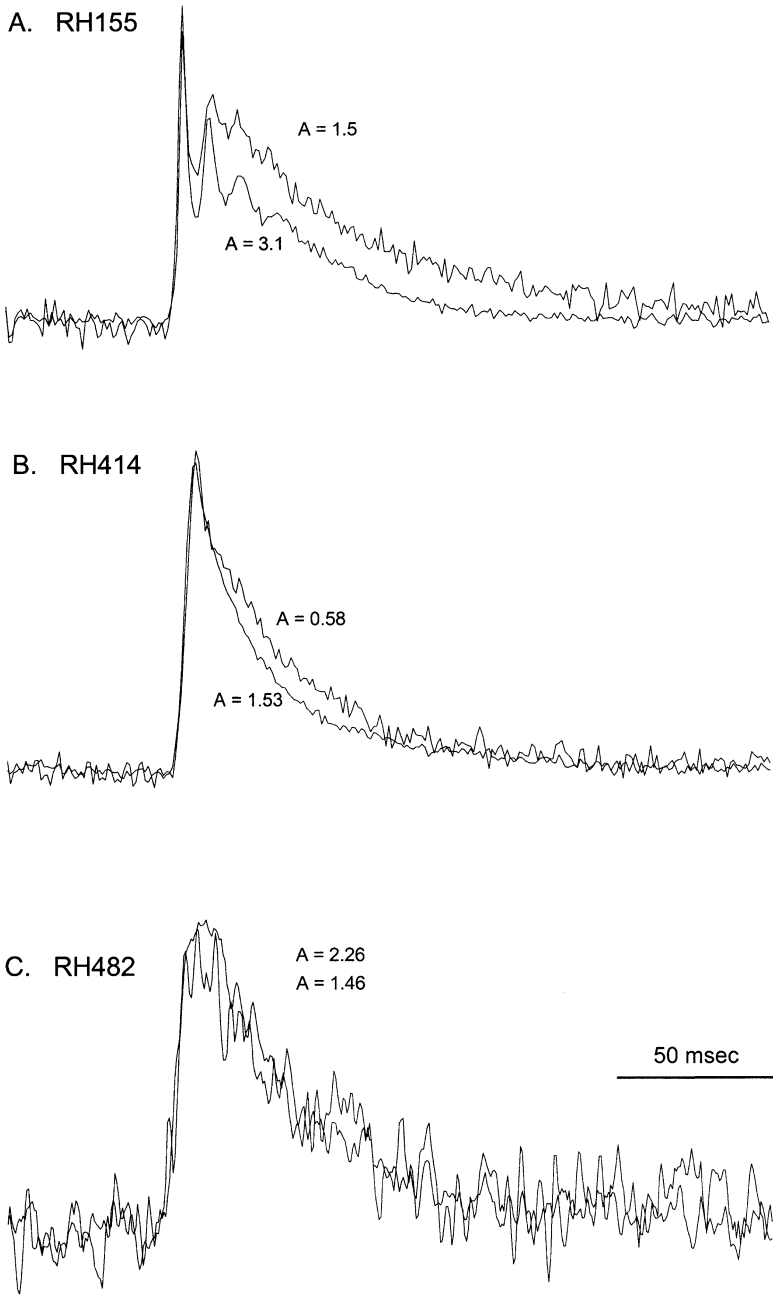

Fig. 5. Comparison of signals from heavily and moderately stained slices. Slices stained for varying times > 15 minutes (longer than in Fig. 4). The dye *OD* (*A*) provides a relative index of staining. The comparison of heavily and moderately stained slices indicates that RH155 has a strong pharmacological action and that RH414 and RH482 do not. RH155 and RH414 are single trials, and RH482 is an average of 6.

For a cell culture preparation where A may be only $\sim$0.01, this equation gives 5. Thus, fluorescence imaging is advantageous in cell culture, as pointed out by Waggoner and Grinvald (1977), using different arguments.

Results

Dye Tests

We examined three dyes in this study, RH155, RH414, and RH482. In lightly stained slices comparisons between field potentials and dye-absorbance signals from the same location (stratum radiatum of CA1, with stimulus $\sim$200 μm away in the same layer) showed the same response for all three dyes (Fig. 3). The field potential (inverted in sign and normalized to facilitate comparison) was briefer than the dye signal, with the negativity coinciding with the rising phase of the dye signal. This indicates that the depolarizations reported by the dye signals result from strong inward currents that give rise to the field potential. The decay of the dye signals presumably results from weaker outward currents so that positive-going field potential is harder to see. Small variations in the three decays

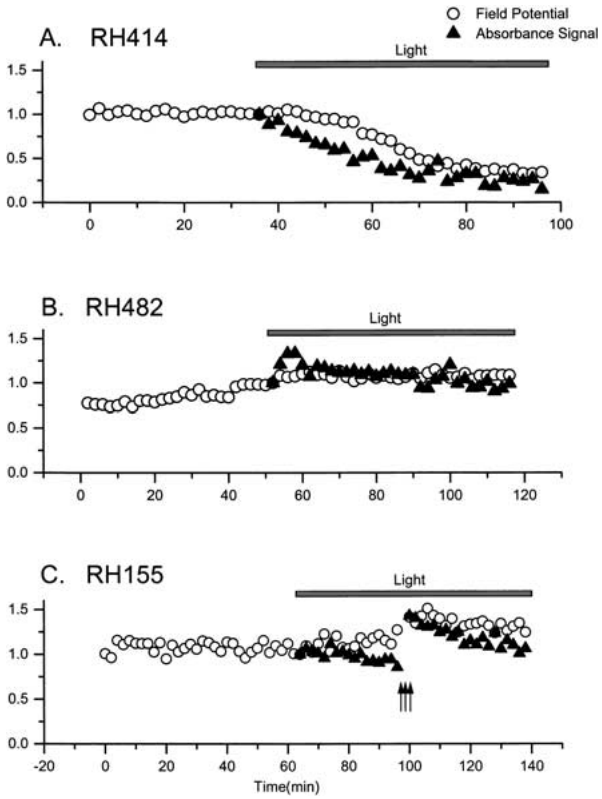

Fig. 6. Phototoxicity of RH414 (*A*), RH482 (*B*), and RH155 (*C*). Toxicity was tested by recording field potentials in the absence of illumination, and then initiating optical recordings at the bar. Optical recordings were made at two-minute intervals during which slices were illuminated for 4.8 sec (average of six trials with 0.8 sec of exposure per trial). All signals were normalized to their values immediately prior to the onset of optical recording. The decline in signals from an RH414-stained slice indicates that this dye is phototoxic. Field potentials remained unchanged in an RH482-stained slice. Field potentials in an RH155-stained slice remained flat after the onset of illumination, and were potentiated by high frequency trains applied at the arrows.

shown may reflect slight variations between recording sites or dye pharmacological activity (examined below). The association of a negative field potential with the depolarizing component of a dye signal has been noted in other studies in which the two were compared (Demir et al., 1998, 2002; Jin et al., 2002).

The theoretical analysis indicated that relatively high staining levels optimize the signal-to-noise ratio, raising concerns about pharmacological actions. We tested for pharmacological actions of the three dyes employed in this study in both lightly-stained and heavily stained slices. We first compared field potentials in unstained slices and in slices stained for ~15 minutes (light staining). Normalizing these signals to their maxima showed that the dyes had little if any effect on the time course of electrically-evoked field potentials (Fig. 4). The only differences were in latency, and this reflects variations in the distance between the recording and stimulation sites in the different experiments.

To obtain higher dye ODs, slices were stained for longer times. Heavier RH155 staining gave rise to signals with a complex multiphasic character, suggesting that higher levels of this dye have a pharmacological action (Fig. 5). Longer staining periods with RH414 and RH482 gave signals with essentially the same time course as shorter periods (Fig. 5*B* and *C*), indicating that these dyes have less pharmacological activity.

Aside from pharmacological actions, voltage-sensitive dyes can be phototoxic (Cohen & Salzberg, 1978; Salzberg, 1983; Grinvald et al., 1988; Jin et al. 2002). Phototoxicity was assessed by recording a baseline of field potentials in stained slices for up to one hour in the absence of illumination. Optical recording was then initiated at 2 minute intervals. With RH414, the onset of illumination initiated a steady decline in field potentials. The absorbance signals also declined (Fig. 6*A*), and the decline in the field potential followed the decline in absorbance signal by a few minutes. Thus, RH414 is phototoxic, and this toxicity increased with illumination strength. When illuminated with a 300 W bulb through an objective with an *NA* of 0.95, field potentials and fluorescence signals declined much more rapidly (*data not shown*).

By contrast, phototoxicity could not be detected using the absorbance dyes RH155 and RH482 (Fig. 6*B* and *C*). With RH482, field potentials and dye signals were flat. The signal of RH155 declined slightly, but since the field potential remained flat, this can be explained as washout of dye during perfusion with aCSF, as noted by Momose-Sato et al. (1999). After 32 minutes of simultaneous optical and field-potential recording with RH155, three tetanic trains were applied to induce long-term potentiation of synaptic transmission. This produced an increase in both the dye signal and field potential.

Optimization of Signal-to-Noise Ratio

Because of the similar time courses of RH414 signals in heavily-stained and lightly-stained slices, we selected this dye to evaluate the effect of dye concentration within the framework of the above theoretical analysis. Only two or three recordings were made from each slice so that the phototoxicity described above would not be a problem. Stimulus-evoked absorbance and fluorescence signals were recorded in the molecular layer of the dentate gyrus. These signals are a mixture of monosynaptic responses to the perforant path and disynaptic responses to hilar mossy cells (Jackson & Scharfman, 1996). The filters for absorbance and fluorescence were switched, as indicated in Methods and Fig. 1. Responses to 100 μA 200 μs stimulus currents were normalized to resting light intensity and plotted versus *A* (Fig. 7*A*).

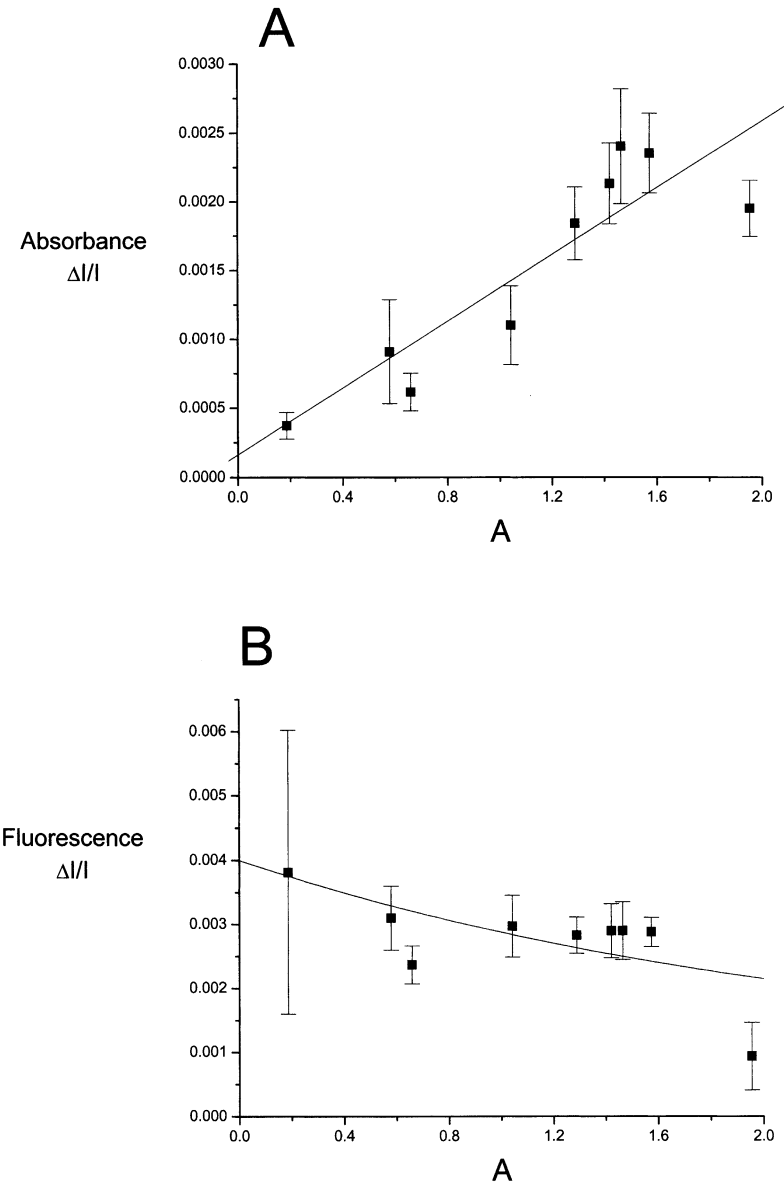

Fig. 7. Normalized changes in light intensity versus *OD* (denoted as *A*). Slices were stained with RH414 for varying periods of time to obtain different levels of absorbance. (*A*) The absorbance signal plot is well fitted by a line through the origin, consistent with Eq. 6. (*B*) The fluorescence signal is plotted versus *A* together with a plot of Eq. 11 with $S = 2$ and scaled to 0.004. All signals were recorded in the molecular layer of the dentate gyrus, with stimulation (100 μA, 200 μs) in the crest. Each point is an average of 10-trial averages from ~5 slices with one or two measurements per slice. In each experiment, fluorescence and absorbance changes were recorded from the same site.

The dependence of the absorbance signal on *A* was linear, as predicted by Eq. 6. The dependence of fluorescence on *A* is shown in Fig. 7*B*. The theoretical plot of Eq. 11 for $S = 2$ appears to be in reasonable agreement with experiment but we were concerned with how flat the plot was over the range $A = 0.5$–1.6 (7 points). The signals at low *A* were very variable, as indicated by the very large standard error of the lowest point (mean of 7 measurements). Excluding two anomalously high values from one slice leads to a value that falls well below the theoretical curve. Thus, despite the appearance of qualitative agreement between theory and experiment in Fig. 7*B*, we would like to leave open the possibility that unknown factors not included in our theory could influence the dependence of fluorescence $\Delta I/I$ signals on *A*.

Similar experiments were performed with RH155 before we noticed its pharmacological activity. It is interesting to note that the plot of $\Delta I/I$ versus *A* was linear for low *A*, but leveled off at higher values (*data not shown*). This saturation disagrees with the prediction of Eq. 6 and probably reflects an inhibition of responses with high staining densities. Thus, the discrepancy can be attributed to the pharmacological activity of the dye. In fact, plots of this kind could be very useful in assessing pharmacological actions. The fact that the plot with RH414 in Fig. 7*A* is linear and goes through the origin argues against pharmacological activity.

The experimental signal-to-noise ratios for absorbance and fluorescence are plotted in Fig. 8. Each plot has a maximum, reflecting the staining level that optimizes these measurements. To determine the optimum from these experiments the data were fitted to the expression $Y \cdot A \cdot e^{-A/Z}$, where *Y* and *Z* are free parameters. This expression has a maximum at $A = Z$.

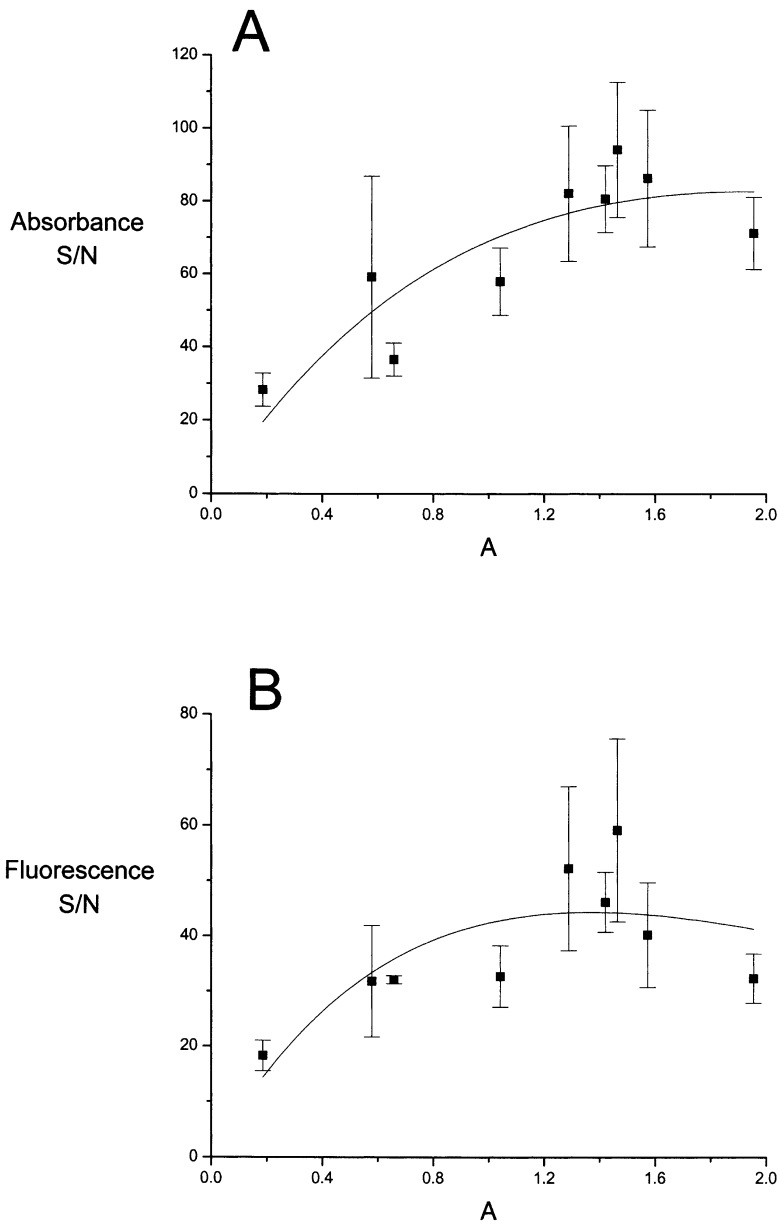

Fig. 8. Signal-to-noise ratio versus dye *OD* (denoted as *A*). The noise was estimated from the RMS at the beginning or end of a trace, corrected as necessary for linear drift. The plot was from the same data set used for Fig. 7. The solid curves are fits of $YAe^{-A/Z}$, which has a maximum at $A = Z$. $Z = 1.9 \pm 0.6$ for (*A*) and 1.3 ± 0.4 for (*B*). Note that the signal-to-noise ratio is generally higher for absorbance than fluorescence.

For the fit to fluorescence data we determined $Z = 1.3 \pm 0.4$, and for the fit to absorbance data we determined $Z = 1.9 \pm 0.6$. The value for fluorescence agrees with the range of maxima of the theoretical curves plotted in Fig. 2*B*. The value for absorbance is indistinguishable from the value of 2 predicted by Eq. 8. The maximum signal-to-noise ratio for absorbance measurements was about 1.5 times higher than that for fluorescence measurements. The theoretical analysis predicted a factor of 1.4 for $S = 2$ and 2.3 for $S = 1$. S values generally ranged from one to two for these slices.

The analysis in Fig. 8 allowed us to estimate the maximal signal-to-noise ratio for an absorbance experiment with RH414 as 83 (computed from the parameters of the fitted curve). This maximum is realized for a fairly broad range of values of $A >$ 1.2. The relevant conditions here were that we used a 5× objective with an *NA* of 0.25, and that 10 responses were averaged. Slices stained with RH482 with a dye *OD* of ~2 gave signal-to-noise ratios of 55 ± 7 under the same conditions (9 measurements from 5 slices).

Discussion

This study makes a number of technical points about the use of voltage-sensitive dyes. One major point is that staining levels can be optimized for the detection of signals using fluorescence and absorbance dyes. To optimize the signal-to-noise ratio for absorbance the staining conditions should be adjusted so that $A = 2$,

meaning that the dye absorbance reduces the recorded light intensity to 13.5% of that expected from the same tissue without staining. To optimize the signal-to-noise ratio for fluorescence experiments the staining conditions should be adjusted so that $A \sim 1$, meaning that dye absorbance reduces the light intensity to 36%. Although the precise optimum for fluorescence varies somewhat depending on scattering and intrinsic absorbance, in practice the variation in signal-to-noise ratio varies insignificantly in the neighborhood of a broad maximum near $A = 1$. These optima were derived theoretically and confirmed experimentally for the dye RH414. They should therefore be useful guidelines in designing voltage-imaging experiments. In comparing fluorescence and absorbance signals within the same experiment, absorbance signals were generally better, as is widely recognized for voltage imaging in thick preparations (Cohen & Lesher, 1986; Grinvald, 1988; Wu et al., 1998; Jin et al., 2002). The advantage of absorbance was relatively modest, and in qualitative agreement with the theoretical prediction.

An important point made here is that normalizing a change in signal to the resting light intensity, taking $\Delta I/I$, does not provide a good measure of the change in the mean extinction coefficient of the dye in the imaged region. If all conditions are identical except for the dye OD, $\Delta I/I$ will be proportional to the dye OD. To convert $\Delta I/I$ to a change in extinction coefficient, one must divide by the OD. A convenient procedure for measuring the OD was introduced here, and using it to make the appropriate correction will remove one significant source of variability from voltage-imaging data.

For fluorescence data the procedure for converting $\Delta I/I$ is not so straightforward. Theoretical analysis indicates that this quantity should decline with increased staining. One could calculate the appropriate factor from Eq. 11 based on measurements of S and A, and use it to convert $\Delta I/I$ to a fractional change in the extinction coefficient. However, the better signal-to-noise ratio and easier procedure for making the correction with absorbance leaves little incentive to use fluorescence dyes in thick preparations.

In closing, we note that the widely used absorbance dye RH155 was found to have pharmacological activity and the widely used fluorescent dye RH414 was found to be phototoxic. Fluorescent dyes are generally found to have greater phototoxicity than absorbance dyes and this is a significant advantage of absorbance over fluorescence (Ross et al., 1977; Gupta et al., 1981). The signal-to-noise ratio was very high in absorbance measurements with RH414 stained to an OD of $\sim$2, making this the method of choice for short-term experiments. For long-term experiments RH482 is preferred (Momose-Sato et al., 1999; Jin et al., 2002). Its lower signal-to-noise ratio is offset by its excellent stability.

Acknowledgments. We thank Larry Cohen for useful discussions and comments on this manuscript. This research was supported by NS30016 from NIH.

References

Cohen, L.B., Lesher, S. 1986. Optical monitoring of membrane potential: methods of multisite optical measurement. *Soc. Gen. Physiol.* Series **40:**71–99

Cohen, L.B., Salzberg, B.M. 1978. Optical measurement of membrane potential. *Rev. Physiol. Biochem. Pharmacol.* **83:**35–88

Demir, R., Gao, B.X., Jackson, M.B., Ziskind-Conhaim, L. 2002. Interactions between multiple rhythm generators produce complex patterns of oscillations in the developing spinal cord. *J. Neurophysiol.* **87:**1094–1107

Demir, R., Haberly, L.B., Jackson, M.B. 1998. Voltage imaging of epileptiform activity in slices from rat piriform cortex: onset and propagation. *J. Neurophysiol.* **80:**2727–2742.

Fluhler, E., Burnham, V.G., Loew, L.M. 1985. Spectra, membrane binding and potentiometric responses of new charge shift probes. *Biochemistry* **24:**5749–5755

Grinvald, A., Frostig, R.D., Lieke, E., Hildesheim, R. 1988. Optical imaging of neuronal activity. *Physiol. Rev.* **68:**1285–1366

Gupta, R.K., Salzberg, B.M., Grinvald, A., Cohen, L.B., Kamino, K., Lesher, S., Boyle, M.B., Waggoner, A.S., Wang, C. H. 1981. Improvements in optical methods for measuring rapid changes in membrane potential. *J. Membrane Biol.* **58:**123–137

Jackson, M.B., Scharfman, H.E. 1996. Positive feedback from hilar mossy cells to granule cells in the dentate gyrus revealed by voltage-sensitive dye and microelectrode recording. *J. Neurophysiol.* **76:**601–616

Jin, W., Zhang, R.-J., Wu, J.-Y. 2002. Voltage-sensitive dye imaging population neuronal activity in cortical tissue. *J. Neurosci. Meth.* **115:**13–27

Kamino, K. 1991. Optical approaches to ontogeny of electrical activity and related functional organization during early heart development. *Physiol. Rev.* **71:**53–91

Loew, L., Cohen, L.B., Salzberg, B.M., Obaid, A.L., Bezanilla, F. 1985. Charge-shift probes of membrane potential. *Biophys. J.* **47:**71–77

Momose-Sato, Y., Sato, K., Arai, Y., Yazawa, I., Mochida, H., Kamino, K. 1999. Evaluation of voltage-sensitive dyes for long-term recording of neural activity in the hippocampus. *J. Membrane Biol.* **172:**145–157

Ross, W.N., Salzberg, B.M., Cohen, L.B., Grinvald, A., Davilla, H.V., Waggoner, A.S., Chang, C.H. 1977. Changes in absorbtion, fluorescence, dichroism, and birefrigence in stained axons: Optical measurement of membrane potential. *J. Membrane Biol.* **33:**141–183

Salzberg, B.M. 1983. Optical recording of electrical activity in neurons using molecular probes. *In:* Current Methods in Cellular Neurobiology p. 139–187. Barker, J.L., McKelvy, J.F., editors. John Wiley & Sons, New York.

Shoham, D., Glaser, D.E., Arieli, A., Kenet, T., Wijnbergen, C., Toledo, Y., Hildesheim, R., Grinvald, A. 1999. Imaging cortical dynamics at high spatial and temporal resolution with novel blue voltage-sensitive dyes. Neuron **24:**791–802.

Skoog, D.A. 1985. Principles of Instrumental Analysis. Saunders College Publishing, Philadelphia

Waggoner, A.S. 1979. Dye indicators of membrane potential. *Annu. Rev. Biophys. Bioengin* **8:**47–68

Waggoner, A.S., Grinvald, A. 1977. Mechanisms of rapid optical changes of potential sensitive dyes. *Ann. New York Acad. Sci.* **303:**217–241

Wu, J.Y., Cohen, L.B. 1993. Fast multisite optical measurements of membrane potential. *In:* Fluorescent and Luminescent Probes for Biological Activity. p 389–404. Mason, W.T., editor. London: Academic Press.

Wu, J.Y., Lam, Y.W., Falk, C.X., Cohen, L.B., Fang, J., Loew, L., Prechtl, J.C., Kleinfeld, D., Tsau, Y. 1998. Voltage-sensitive dyes for monitoring multineuronal activity in the intact central nervous system. *Histochem. J.* **30:**169–187